The Amino Acid Sequence Coded by the Rarely Expressed Exon 26A of Human Elastin Contains a Stable β-Turn with Chemotactic Activity for Monocytes[†]

Faustino Bisaccia, Maria Antonietta Castiglione-Morelli, Susanna Spisani,[‡] Angela Ostuni, Augusto Serafini-Fracassini, Alfonso Bavoso, and Antonio Mario Tamburro*

Department of Chemistry, University of Basilicata, Potenza, Italy

Received February 2, 1998; Revised Manuscript Received May 7, 1998

ABSTRACT: The structural and biological properties of the amino acid sequence coded by the rarely expressed exon 26A of human elastin were investigated. The C-terminal portion of this sequence, corresponding to residues 600−619 of human tropoelastin, REGDPSSSQHLPSTPSSPRV and three shorter derived peptides, LREGDPSS, SSSQHLPS, and LPSTPSSP, were synthesized and studied. Spectroscopic analyses by CD and NMR have identified a type II β-turn within the sequence REGD of the octapeptide LREGDPSS. This structural motif was found also in the tetrapeptide REGD in both trifluoroethanol and water. The CD spectrum of the tetrapeptide REGD in trifluoroethanol was consistent with a pure type II β-turn. A high chemotactic activity for monocytes was exhibited by the structured peptides REGD (CI 0.90 at 10^{-7} M) and LREGDPSS (CI 0.80 at 10^{-11} M), at variance with the unfolded peptides LPSTPSSP and SSSQHLPS, suggesting that this activity is strictly correlated with folded structures. Because the exon 26A of human elastin is expressed in the neointima of hypertensive pulmonary arteries, and macrophages are present in this pathologic tissue [Liptay et al. (1993) *J. Clin. Invest. 91,* 588−594], the chemotactic activity for human monocytes reported in this paper is consistent with an active role played by the exon 26A in inducing the migration of the monocyte/macrophage cells to the neointima.

The elastic properties of several vertebrate tissues such as lung, skin, and large blood vessels are mainly due to the presence of elastic fibers within their extracellular matrix. Elastin, the major component of these fibers, is synthesized by mesenchymal cells as a soluble precursor, tropoelastin, which undergoes post-translational modifications leading to the formation of specific cross-links that join together several tropoelastin chains (*1*−*2*). Besides being responsible for the elastic properties of connective tissue, tropoelastin and some soluble derivatives of elastin have now been demonstrated to also exhibit biological activities and to able to modify cellular behavior (*3*−*4*). The identification of the sequences which exhibit biological activity and the study of their structure are important steps in the elucidation of the role that they may play in the regulation of biological events in both pathological and physiological conditions. Presently, several elastin-derived peptides have been identified which show chemotactic activity for fibroblasts, monocytes, and tumor cells (*5*−*7*).

The complete amino acid sequences of human, bovine, chicken, rat, sheep, and mouse tropoelastin have been deduced from cDNA sequences (*8*−*13*). The genomic DNA of human and bovine elastin have also been characterized (*14*); nucleotide sequencing has revealed that functionally distinct cross-linking and hydrophobic domains of elastin are encoded in separate exons. Furthermore, alternative splicing of a single primary transcript was demonstrated (*8*, *9*, *15*) which could explain the identification of different forms of tropoelastin in different species. At present, it is not known whether the splicing pattern is developmentally regulated or tissue-regulated and whether there are functional differences between different tropoelastin molecules.

In human elastin, at variance with other species, there is an exon (26A) which is involved in alternative splicing and is rarely expressed (*8*). In contrast to the rest of the protein, the sequence coded by this exon is rich in charged and polar amino acids (Arg, Asp, Glu, Ser) and contains the only His residue of the whole macromolecule. Only limited information is presently available on the properties of elastin containing this additional sequence.

[†] This work was supported by grants from MURST, LAMI, and CNR.

* To whom correspondence should be addressed. Department of Chemistry, University of Basilicata, via N. Sauro 85, 85100 Potenza, Italy. Tel: +39-971-474219. Fax: +39-971-474223. E-mail: tamburro@unibas.it.

[‡] Current Address: Department of Biochemistry and Molecular Biology, University of Ferrara, Ferrara, Italy.

[1] Abbreviations: NMR, nuclear magnetic resonance; CD, circular dichroism; fMLP, *N*-formylmethionylleucylphenylalanine; Fmoc, 9-fluorenylmethyloxycarbonyl; DCC, dicyclohexylcarbodiimide; HOBt, 1-hydroxybenzotriazole; HMP, *p*-hydroxymethylphenoxymethylpolystirene resin; $DMSO_{d6}$, perdeuterated dimethyl sulfoxide; TFE_{d3}, perdeuterated trifluoroethanol; NOESY, 2D nuclear Overhauser effect spectroscopy; $^3J_{NH\alpha}$, vicinal coupling constant between NH and α protons; TOCSY, 2D total correlation spectroscopy; ROESY, 2D rotating frame Overhauser spectroscopy; $d_{NN(i,j)}$, $d_{\alpha N(i,j)}$, $d_{\alpha\delta(i,j)}$, intramolecular distance between the protons NH and NH, $C^{\alpha}H$ and NH, and $C^{\alpha}H$ and $C^{\delta}H$ on residues i and j; KRPG, Krebs−Ringer phosphate containing 0.1% w/v glucose; SE, standard error; SPDP, *N*-succinimidyl 3-(2-pyridyldithio) propionate; BSA, bovine serum albumine; PBS, phosphate buffer saline; OPD, *o*-phenylenediammine; CI, chemotactic index; rmsd, root-mean-square deviation; K_{dc}, force constant for distance constraints.

S0006-2960(98)00256-6 CCC: $15.00
Published on Web 07/17/1998

Bedell-Hogan et al. (*16*) found that recombinant tropoelastin in which the amino acid sequence coded by exon 26A is present shows a K_m for lysyl oxidase lower than that of tropoelastin devoid of this sequence. Furthermore, a prediction method of immunogenicity suggests the presence of a linear epitope within this sequence (*17*). Finally, it has been reported that exon 26A is expressed in the neointima of hypertensive pulmonary arteries (*18*).

To shed light on the functional role of exon 26A, we have undertaken a systematic study of the conformational and biological properties of the encoded peptide sequence of which we report the results obtained with the C-terminal region (REGDPSSSQHLPSTPSSPRV), corresponding to residues 600−619 of human tropoelastin. We have found that this sequence exhibits immunogenic properties and adopts a stable type II β-turn structure which correlates well with its high chemotactic activity for monocytes.

MATERIALS AND METHODS

Peptide Syntheses. The synthesis of the peptides CREGDPSSSQHLPSTPSSPRV, REGDPSSSQHLPSTPSSPRV, LREGDPSS, SSSQHLPS, LPSTPSSP, and REGD was performed on a solid-phase automatic peptide synthesizer, Applied Biosystems model 431A. The Fmoc/DCC/HOBT strategy was used. The peptides were debound from the HMP resin with 95% trifluoroacetic acid, dried, and purified by HPLC using a semipreparative C18 reversed-phase column. Peptide purity was assessed by NMR in $DMSO_{d6}$ and by sequence analysis in an Applied Biosystems 491 pulsed-liquid protein sequencer.

Human recombinant tropoelastin and human α-elastin were kindly supplied by Professors J. Rosenbloom and D. Daga, repectively.

CD Spectra. Circular dichroism spectra were recorded in a cylindrical cell, 0.1 cm path length, with a JASCO 600A automatic circular dichrograph. Sample concentrations were 0.1 mg mL^{-1}. All spectra were smoothed using the Fourier transform routine of the J-600A. Baseline spectra of the appropriate solvents were subtracted. Data were expressed in terms of $[\theta]$, the molar ellipticity, in units of deg cm^2 $dmol^{-1}$.

NMR Spectra. NMR measurements were carried out on 300 and 500 MHz AMX Bruker spectrometers using a 2.5 mM sample of the octapeptide and a 6.3 mM sample of the tetrapeptide in 70% TFE_{d3} (Cambridge Isotopes Laboratories, Cambridge, MA)/30% ^1H_2O. Chemical shifts were measured relative to the methyl resonance of 4,4-dimethyl-4-silapentane-1-sulfonate (0 ppm).

2D NMR spectra were acquired at 280 and 295 K in phase sensitive mode (TPPI). The water resonance was suppressed by presaturation for 1.3 s and during the mixing time of NOESY experiments. 2D TOCSY spectra were acquired using the TOWNY composite pulse cycle (*19*). Mixing times used were 69 ms for the TOWNY, 300 and 500 ms for the NOESY (*20*), and 200 ms for the ROESY experiments (*21*), respectively.

All experiments were recorded with 2048 data points in the acquisition domain and 512 data points in t_1. The t_1 domain was zero-filled to 2048 points prior to Fourier transformation. The data were weighted in t_2 with a $\pi/8$ shifted sine-bell window and in t_1 with a $\pi/4$ shifted sine-bell window, respectively.

Processing of the 500 MHz data was performed on a IRIS Indigo using UXNMR/P. NOE spectra were integrated and calibrated by the AURELIA software (*22*).

1D spectra were recorded at 5 K increments between 295 and 315 K, with 16 000 complex data points and using zero-filling for processing.

Structure Calculations. From the 300-ms NOESY spectrum of the octapeptide at 295 K a total of 40 NOEs were collected (26 intraresidual and 14 sequential NOEs). Distance upper limits were calculated by the cross-diagonal peak ratio method (*23*, *24*), to which an additional correction of 0.2 Å was made in order to take into account the estimated error on the calculated distances. The correlation time (0.89 ns) used in the calculation was computed using the distance between the amide terminal protons (1.8 Å). Stereospecific assignments were obtained for the β-proton pairs of Arg^2, Glu^3, and Asp^5 using the HABAS program (*25*). When no stereospecific assignment was possible for β-methylene protons, distance constraints were corrected for pseudoatom representation (*26*); for methyl groups of Leu^1 an additional correction of 0.5 Å was added to take into account the multiplicity.

3D structures were generated consistently with the NMR data by combined use of distance geometry calculations, performed with the DIANA program (*27*), and energy minimization. The variable target function was changed according to the standard strategy from level 1 to level 8. A total of 50 starting structures were generated from random choices of dihedral angles, and the best 30 structures in terms of distance violations were chosen for further refinement by means of restrained energy minimization with the package AMBER, version 4.1 (*28*). Five-thousand steps of restrained energy minimization (K_{dc}= 20 kcal mol^{-1} $Å^{-2}$) with a combination of steepest descent and conjugate gradient algorithms were applied to each structure. Graphical representation and rmsd analysis between energy minimized structures were carried out with the program MOLMOL (*29*).

Generation of Rabbit Anti-Peptide Antibodies. The peptide CREGDPSSSQHLPSTPSSPRV, corresponding to the sequence 600−619 of human tropoelastin with an added cysteine at the N-terminal position, was coupled to bovine serum albumin through the SH group of this cysteine using *N*-succinimidyl 3-(2-pyridyldithio) propionate (SPDP) (*30*). The yield of the coupled peptide was determined spectrophotometrically from the pyridine-2-thione released. The BSA−peptide conjugate was dialyzed against PBS to remove the excess SPDP and unbound peptide. Aliquots of the conjugate, containing 100 μg of coupled peptide, in 0.5 mL of PBS were supplemented with 0.5 mL of complete Freund's adjuvant and used to immunize male New Zealand white rabbits as previously described (*31*).

Antibody Assay by ELISA. The ability of the antiserum to react with the synthetic peptide, its BSA conjugate, and recombinant human tropoelastin, containing the sequence coded by exon 26A, was tested by ELISA on microtitration polystyrene plates. Aliquots, 200 μL each, of the protein/peptide samples dissolved in PBS were added to the wells. After overnight incubation at 4 °C, the wells were emptied and washed with PBS. They were then filled with 200 μL of a 1% skimmed milk solution in PBS, and the plate was

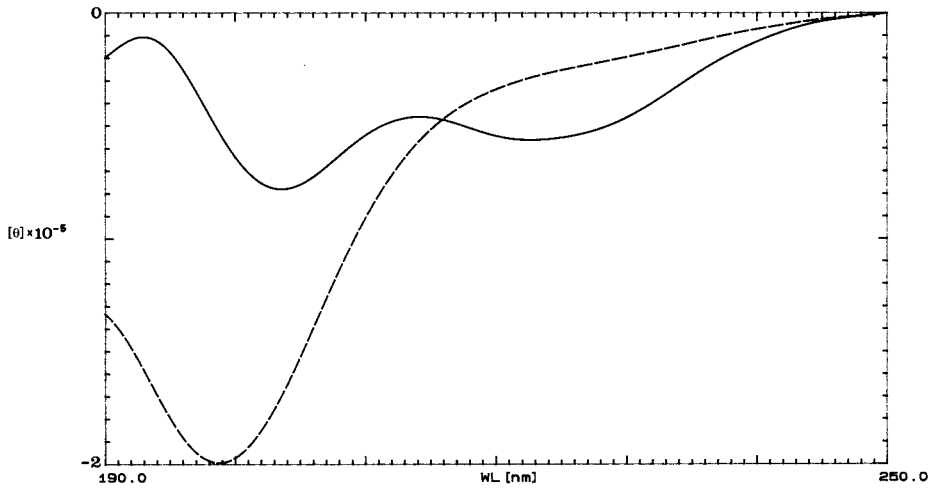

FIGURE 1: CD spectra of REGDPSSSQHLPSTPSSPRV in water (- - -) and TFE (—).

allowed to stand for 1 h at room temperature for saturation of binding sites. After washing the plate with PBS-Tween, 200 μL of antiserum diluted with PBS-Tween was added to the wells, and the plate was incubated at room temperature for 2 h. The plate was washed with PBS-Tween, and 200 μL of a solution of horseradish peroxidase-conjugated anti-rabbit Ig, diluted 2000-fold with PBS-Tween in PBS-Tween, was added to each well. After an additional 2 h of incubation at room temperature followed by washings, each well was filled with 200 μL of a solution containing 0.8 mg/mL of *o*-phenylenediammine (OPD) in 50 mM phosphate/citrate buffer, pH 5.0, with 0.03% sodium perborate. The peroxidase reaction was left to develop for 1 h in the dark at room temperature and then stopped by addition of 50 mL of 2 M H_2SO_4. The absorbance at 450 nm of the reaction medium was recorded with an automatic reader.

Western Blot Assay. Besides ELISA, the Western blot technique (*32*) was used to test the reactivity of the antipeptide antisera against the peptide-BSA conjugate and recombinant human tropoelastin containing the sequence coded by exon 26A. Ten micrograms of the sample was run on polyacrylamide gel electrophoresis according to Laemnli (*33*). After electroblotting (*31*), the nitrocellulose sheets were treated with the antiserum as indicated in the legend to Figure 6, and then incubated with horseradish peroxidase-conjugated anti-rabbit Ig. The immunoreaction was detected by the peroxidase reaction performed with 20 mL of a mixture of 4-chloro-1-naphthol (0.05% w/v), methanol (16% v/v), and BSA (0.5%w/v) in a medium containing 0.14 M phosphate (pH 7.0) with the final addition of 10 μL of 30% H_2O_2.

Migration Assay of Monocytes. Mononuclear cells were isolated from heparinized blood of normal human volunteers by sedimentation over Ficoll-Paque (Pharmacia, Uppsala Sweden). Cells were washed twice and resuspended in KRPG (Krebs−Ringer phosphate containing 0.1% w/v glucose, pH 7.4). Cell migration was performed in a modified Boyden chamber, using a 48 multiwell chemotaxis chamber (Neuro Probe, Inc., Milano, Italy) in which the distance in micrometers covered by the migrating cell leading-front was assessed using the method of Zigmond and Hirsch (*34*).

To test the chemokinetic effect, the peptides were added to both top and bottom compartments separated by an 8 μm pore size filter (Millipore, Bedford MA), at final concentrations in the range 10^{-12}−10^{-5} M as described elsewhere (*35*). To study the chemotactic activity, each peptide was added to the lower compartment of the chemotaxis chamber at final concentrations in the range 10^{-12}−10^{-5} M. A differential assessment of the effects exerted by the peptides on monocyte chemokinesis and chemotaxis was obtained by checkerboard assay, using different concentration gradients of chemoattractant in the absence or presence of peptides. Peptide stock solutions (10^{-2} M in dimethyl sulfoxide) were diluted in KRPG, containing bovine serum albumin (Orha, Beringwerke, Germany), before use. Data were expressed in terms of the chemotactic index (CI), which is the ratio between the migration toward the test attractant, from which the migration toward the buffer was deducted, and the migration toward the buffer.

Migration in the presence of buffer alone was 35 μm ± 3 SE. In all experiments 10^{-8} M fMLP was used as a peptide control; peak response migration was 68 μm ± 4 SE (CI 0.92 ± 0.03). The nonparametric Wilcoxon test was used in the statistical evaluation of data.

RESULTS

CD Results. Figure 1 shows the CD spectra of REGDPSSSQHLPSTPSSPRV in solvents of different polarity. The peptide has a random conformation in water but appears to acquire a folded structure in apolar solvents; in TFE the large negative trough at 200 nm, characteristic of unordered structures, is sufficiently reduced to become compatible with the coexistence of folded and unfolded structures. To clarify this issue, we have synthesized and analyzed the conformation of three peptides: LREGDPSS, SSSQHLPS, and LPSTPSSP, corresponding to the N-terminal, central, and C-terminal regions, respectively, of the 20-residue peptide. Figure 2 shows the CD spectra of these peptides in TFE. The CD spectra of SSSQHLPS and LPSTPSSP show a large negative band at 198 nm indicative of random conformation. On the other hand, this negative band is completely absent in the CD spectrum of LREGDPSS where the presence of a positive band at 192 nm is indicative of the coexistence of folded peptides, probably in a type II β-turn conformation, and unordered conformers, as suggested by the shoulder at 205 nm. Alternatively, this pattern could

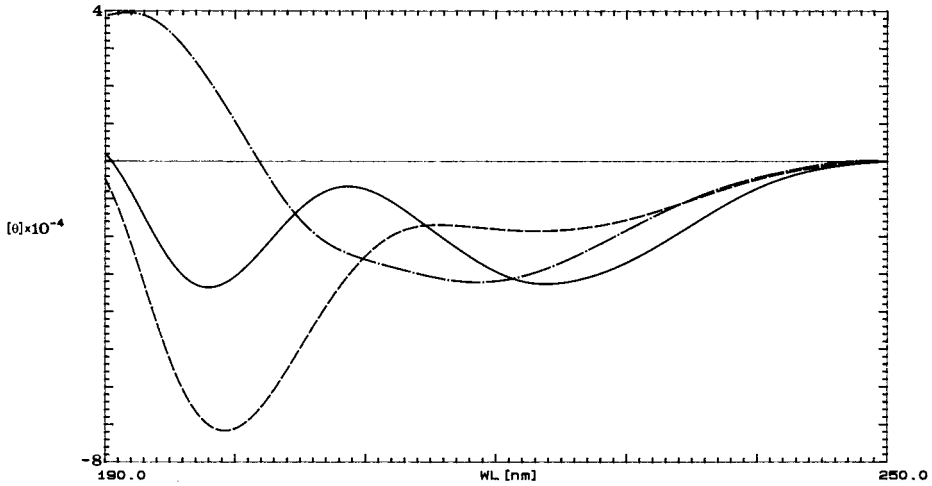

FIGURE 2: CD spectra in TFE of the octapeptides LREGDPSS (− · −), LPSTPSSP (—), and SSSQHLPS (- - -).

arise from the coexistence in the same molecule of ordered segments with others devoid of a stable conformation.

NMR of LREGDPSS

Chemical Shift Assignment. In the peptide examined, different amino acids are present in the sequence only once, with the exception of Ser; consequently, spin system assignments by TOCSY spectra lead directly to sequence-specific assignments (*36*). The deviation of α-H chemical shifts for peptides and proteins from their "random coil" values has commonly been used as an indication of secondary structure (*37*, *38*). They tend to occur downfield of random coil values for residues involved in β-strands or extended secondary structure or upfield in regions of α-helix. The only downfield shift was observed for Asp^5 which is likely to be due to the adjacent Pro, because proline residues frequently have been found to give rise to a shift deviation of the preceding residue α-H (*39*). All other shifts were quite close to their random coil values, and this suggests that if any structure exists in solution this is in equilibrium with a significant proportion of random coil conformations.

Coupling Constants. $^3J_{\alpha H-NH}$ coupling constants,which reflect the ϕ torsion angle, are useful indicators of secondary structure. In fact, $^3J_{\alpha H-NH}$ may be directly used to distinguish between helical ($J < 5$ Hz) or extended conformations ($J >$ 8 Hz). However, conformational flexibility, common in small peptides, results in averaged values of 6−7 Hz, even if significant populations of folded forms are present (*40*). $^3J_{\alpha H-NH}$ values were measured from 1D spectra and are included in Figure 3A.

In many cases, β-turns may be characterized by specific patterns of low and high $^3J_{\alpha H-NH}$ at positions 2 and 3 of the turn (*36*). In this study, however, the relevant $^3J_{\alpha H-NH}$ of the third residue of the β-turn, which is useful to distinguish between a turn of type I ($^3J_{\alpha H-NH} = 9$ Hz) or type II ($^3J_{\alpha H-NH} = 5$ Hz), belongs to a Gly residue and therefore cannot be used to further confirm the presence of a type II β-turn.

Temperature Studies. The temperature dependence of the amide chemical shifts was determined over the range 295−315 K. In all cases, the chemical shift varied linearly with temperature. The temperature coefficients are given in Figure 3A. None of the observed temperature coefficients is in the range expected for strong, intramolecular hydrogen bonds involving amide protons. However, the Asp^5 temperature coefficient (−3.6 ppb/K) falls in an intermediate range (−3 to −4 ppb/K) which has often been interpreted as indicating weakly hydrogen-bonded amide groups.

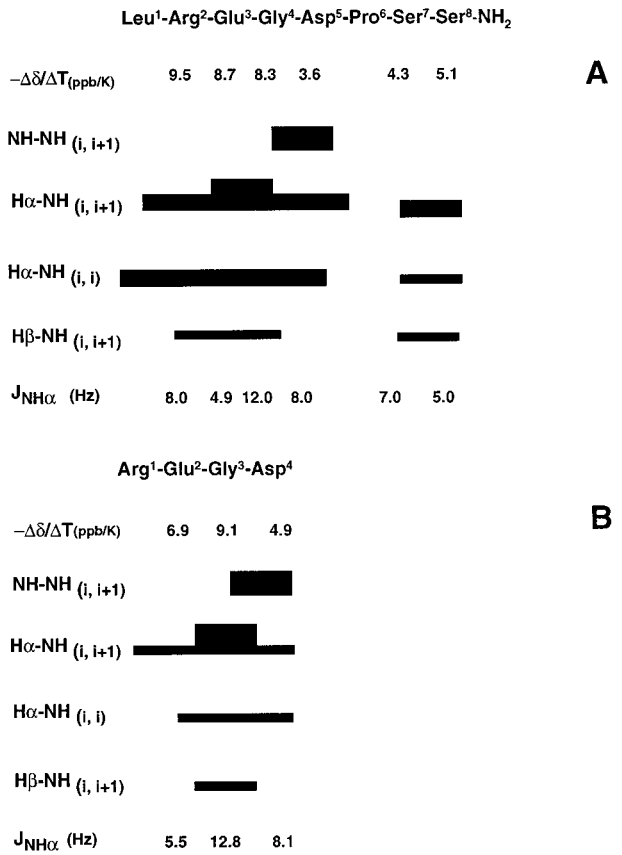

FIGURE 3: Amide proton temperature coefficients ($-\Delta\delta/\Delta T$, ppb/K), NOEs, and $^3J_{NH\alpha}$ coupling constants (Hz) observed for (A) the octapeptide and (B) the tetrapeptide in 70% TFE/30% water. The temperature coefficients were measured in the temperature range 280−295 K. NOE intensities are indicated by the height of the bars. Coupling constants were measured at 295 K; the $^3J_{NH\alpha}$ values of Gly residues are the sum of J_{AX} and J_{BX}.

NOESY Experiments. A large number of CD and NMR studies use TFE as a structure-inducing solvent for peptides. There are many examples where TFE induces helices in peptides that have an intrinsic propensity for helix formation (*40*−*44*). Since our peptides are largely unstructured and

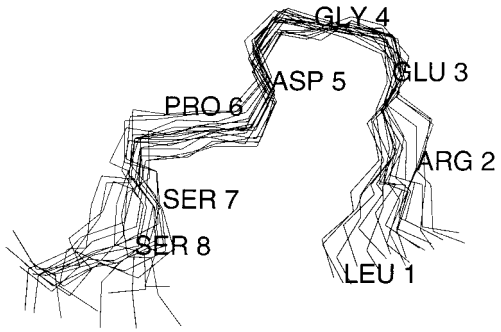

FIGURE 4: Superposition of the 19 lowest energy calculated structures for the octapeptide. Only backbone atoms are shown. The structures are superimposed for minimum rmsd of backbone atoms of residues 2−5.

flexible in aqueous solution but become increasingly structured at higher TFE concentrations, as judged by CD, we decided to use a 70% TFE/30% water mixture for our NMR studies. All the sequential $d_{\alpha N}(i,i+1)$ and $d_{\beta N}(i,i+1)$, as well as the intraresidual $d_{\alpha N}(i,i)$ and $d_{\beta N}(i,i)$ connectivities, are present in the NOESY experiment at 295 K. A summary of the NOE connectivities observed for the octapeptide is presented in Figure 3A. A NOE observed between the Asp^5 α-proton and the Pro^6 δ-protons indicates that the Asp^5-Pro^6 peptide bond is trans. An intense cross-peak is found connecting the Gly^4 amide proton and the Glu^3 α-proton while a strong cross-peak is also observed between the Gly^4 and the Asp^5 amide protons, suggesting that a type II β-turn is adopted by residues 2−5.

A decrease in temperature generally makes the observation of structured conformers more likely (*45*), so NOESY and ROESY experiments were recorded for the octapeptide also at 280 K. Since ROESY experiments are less susceptible to spin-diffusion than normal NOESY experiments, a ROESY spectrum (200 ms mixing pulse) was collected to ensure that none of the structurally relevant NOEs were derived from relayed NOEs or spin diffusion. All the NOE cross-peaks observed in NOESY spectra were observed as ROE cross-peaks. Both experiments confirmed the NOEs already observed at 295 K, consistent with the presence of a type II β-turn spanning residues 2−5.

Structure Calculations of the Octapeptide. A total of 40 distance restraints were derived from NOESY spectra (26 intraresidual and 14 sequential). They were used in distance geometry calculations, performed with the DIANA program (*27*). Energy refinement was then performed to obtain the conformation of the octapeptide which is shown in Figure 4 as a superposition of 19 representative structures of the octapeptide best-fitting residues 2−5. These structures fulfill the structural quality criteria as described in Table 1. The average rmsd of the backbone atoms for all residues is 1.35 ± 0.45 Å and decreases to 0.44 ± 0.23 Å for residues 2−5, while the corresponding values for the heavy atoms are 2.44 ± 0.52 for all residues and 1.81 ± 0.52 for residues 2−5 (Table 1). The hydrogen bond between the amide proton of Asp^5 and carbonyl of Arg^2 is consistently present in all calculated structures.

NMR and CD of REGD

The identification of a β-turn structure within the sequence REGD of the octapeptide prompted us to synthesize the tetrapeptide REGD in order to verify if the type II β-turn is still present in this shortened peptide. The NMR data summarized in Figure 3B seem to confirm the presence of this structural motif. In fact, in the NOESY spectra of the tetrapeptide, the presence of a strong cross-peak between the Gly^3 and the Asp^4 amide protons, together with a cross-peak connecting the Gly^3 amide proton and the Glu^2 α-proton which is stronger than the other dαN cross-peaks, suggests that a type II β-turn conformation may be assumed by the peptide.

$^3J_{\alpha H-NH}$ coupling constants, reported in Figure 3B, are values typical of averaged conformations and indicate a certain degree of conformational flexibility in the tetrapeptide backbone. It would appear that there is a propensity for the peptide to form a turn structure; this is, however, in equilibrium with randomly structured conformations.

This finding is confirmed by the temperature coefficients of the amide protons. Their high values indicate little or no shielding of these protons from the solvent, as instead should occur when species are folded and/or involved in hydrogen bonds. The lowest value is, anyway, that found for Asp, the fourth residue of the turn, which could be involved in hydrogen bond formation with the carbonyl of the first residue. However, it should be noted that the stabilization of a β-turn by a 4 → 1 hydrogen bond is not a requirement for turn formation (*40*).

The CD spectra of REGD in TFE and in the mixed solvent CH_3CN/TFE (Figure 5) are of considerable interest since they are almost perfect examples of type II β-turns acccording to both theoretical and experimental results of Perczel et al. (*46*). The folded structure is still present in the aqueous solution demonstrating the presence of a very stable β-turn.

Antibody Characterization. The reactivity of the antiserum obtained from rabbits immunizated with the peptide CREGDPSSSQHLPSTPSSPRV conjugated to BSA, as described in the Experimental Section, was assayed by ELISA and immunoblotting.

Figure 6 shows that at a 1:2000 dilution the antiserum recognizes the peptide-BSA conjugate, used as antigen, the free peptide, and a recombinant tropoelastin that contains the amino acid sequence coded by exon 26A. It does not recognize bovine α-elastin and carbonic anhydrase. The immunoreaction is dose-dependent up to 0.1 μg of peptide/

Table 1: Analysis of the 19 Best DIANA Conformers of the Peptide LREGDPSS after Restrained Energy Minimization

	av value ± sd	range (min, max)
DIANA target function (Å²)[a]	0.87 ± 0.39	0.49, 1.69
AMBER energy (kcal/mol)	−176 ± 8	−188, −153
residual NOE distance restraint violations (Å)		
$\Sigma_{violations}$	1.30 ± 0.35	0.66, 1.92
maximum	0.45 ± 0.04	0.38, 0.50
rmsd values (Å)[b]		
backbone atoms (N, Cα, C′)		
all residues	1.35 ± 0.45	0.51, 3.69
residues 2−5	0.44 ± 0.23	0.05, 1.58
heavy atoms		
all residues	2.44 ± 0.52	1.13, 4.95
residues 2−5	1.81 ± 0.52	0.74, 3.68

[a] Before energy minimization. [b] Averages and standard deviations are given for the pairwise rmsd values between each of the 19 energy refined DIANA structures and the mean structure.

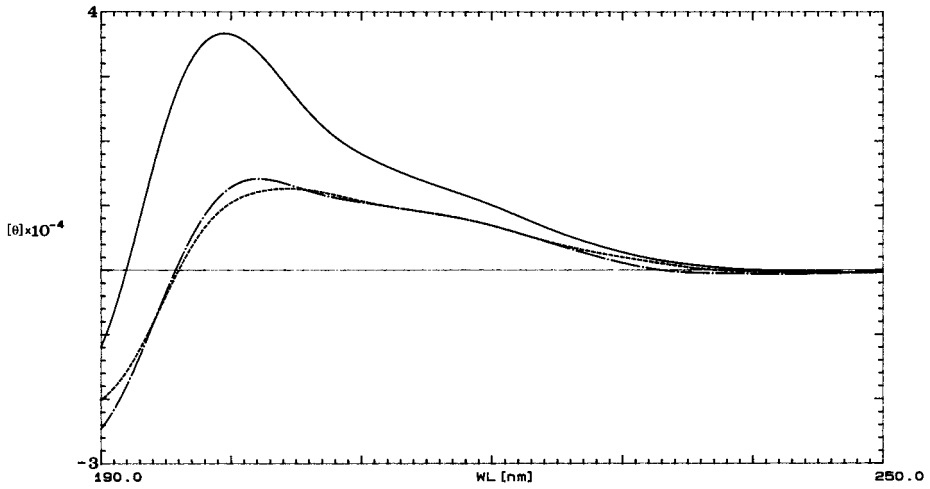

FIGURE 5: CD spectra of the tetrapepdide REGD in different solvents: (—) CH_3CN/TFE 8:2; (— · —) water; (- - -) TFE.

well. In the concentration range used in Figure 6A, recombinant tropoelastin does not reach saturation, probably because of its low molar ratio relative to the peptide.

Figure 6B shows the immunodetection with antiserum of the BSA−peptide conjugate and the recombinant tropoelastin transferred to a nitrocellulose membrane. The extensive denaturation induced by SDS present in the electrophoresis buffer suggests that the antiserum recognizes the epitope in different conformations.

Monocyte Chemotactic Assay. Figure 7 shows the migration of monocytes in response to concentration gradients (ranging from 10^{-12} to 10^{-5} M) of REGDPSSSQHLPSTPSSPRV, LREGDPSS, LPSTPSSP, SSSQHLPS, and REGD. At variance with the unfolded peptides LPSTPSSP and SSSQHLPS, a high chemotactic activity is exhibited by the structured peptides: the tetrapeptide REGD (CI 0.90 at 10^{-7} M) and the octapeptide LREGDPSS (CI 0.80 at 10^{-11} M). The parent peptide REGDPSSSQHLPSTPSSPRV exhibits a value of chemotaxis intermediate between those of the folded and unfolded peptides (CI 0.63 at 10^{-6} M), thus demonstrating that the observed chemotactic activity is strictly correlated with the presence of a folded structure. This finding is in agreement with other reports (*47*, *48*) of chemotactic peptides exhibiting a type II β-turn structure. The dose−response curves are typical of chemoattractants that rise to a peak and then decline as the concentration of the ligand is increased above its optimum value.

To verify the possible presence of chemokinetic activity, that is the migration of cells throughout the filters of the chemotactic chamber in the absence of a gradient, checkerboard analysis was carried out. Data are reported in Table 2. As shown, all peptides exhibit chemokinetic properties besides chemotactic activity, but at different concentrations.

DISCUSSION

The biological significance of alternative splicing may be deduced from the study of the biological and structural properties of the differently spliced protein isoforms. In the case of elastin, this characterization is particularly difficult since elastin performs its mechanical function only after the formation of cross-links that render the protein insoluble. Therefore, the constituent subunits cannot be isolated without subjecting the tissues to degradative processes which have prevented, so far, the isolation of the different isoforms from connective tissue matrices.

At present, some information about the structural and biological properties of different isoforms of tropoelastin has been obtained using recombinant tropoelastin (*16*) and theoretical methods (*17*). In this work we have investigated the structural and biological properties of the sequence REGDPSSSQHLPSTPSSPRV coded by exon 26A of human elastin which is known to be involved in alternative splicing.

The CD spectra of the peptide REGDPSSSQHLPSTPSSPRV suggest the presence of a solvent-dependent folded structure (Figure 1), and the analysis of three shorter constituent octapeptides has allowed us to identify its position and type. In fact, the CD spectrum of the octapeptide LREGDPSS is compatible with the presence of a type II β-turn, albeit coexistent with unordered conformations, while the CD spectra of the other two octapeptides LPSTPSSP and SSSQHLPS are consistent with dominant unfolded conformations (Figure 2).

The presence of a type II β-turn in the peptide LREGDPSS is corroborated by the NMR results: NOESY experiments suggest the presence of a type II β-turn within the sequence REGD of the octapeptide LREGDPSS (Figure 3A), while $J_{\alpha H-NH}$ coupling constants and amide proton temperature studies, although not incompatible with the proposed structure, could not definitely support it. Using the distance restraints derived from NOESY spectra in distance geometry calculations, we have obtained the family of conformations of the octapeptide shown in Figure 4, in which one H-bond between the amide proton of the Asp^5 and the carbonyl of the Arg^2 is consistently present.

This turn is quite stable and is present also in the tetrapeptide REGD, as shown by CD and NMR (Figures 3B and 5). The CD spectra of the tetrapeptide REGD in acetonitrile/TFE and water show the presence of a type II β-turn mixed with random conformations, while the spectrum in TFE agrees with a pure type II β-turn (*46*). At variance with the octapeptide, the NMR data in TFE/water confirm the presence of a type II β-turn but do not show the presence of a H-bond within the β-turn. These data agree with the CD spectrum in water and demonstrate that the β-turn is stable "per se" independently from the presence of the H-bond. Therefore, in the light of the NMR results obtained with the octapeptide LREGDPSS and the tetrapeptide REGD, the CD spectrum of the octapeptide may be interpreted not as due to an equilibrium between folded and unfolded

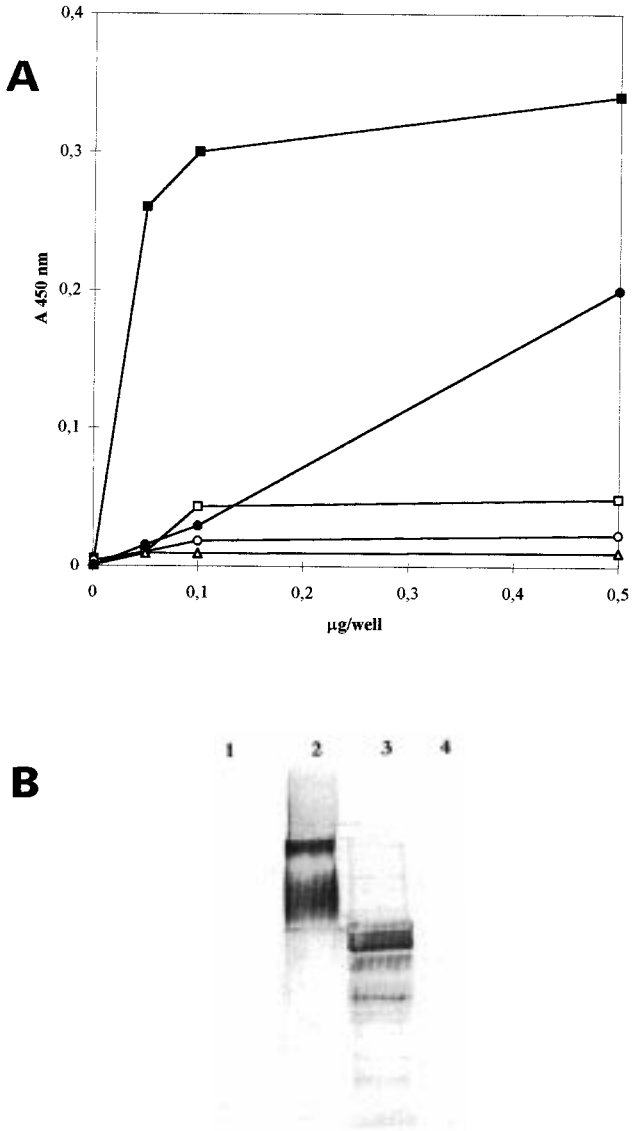

FIGURE 6: (A) Reactivity of anti-CREGDPSSSQHLPSTPSSPRV antiserum assessed by ELISA. Microtiter plates were coated with the CREGDPSSSQHLPSTPSSPRV peptide (■); BSA (□); human tropoelastin (●); bovine α-elastin (○); carbonic anhydrase (△). (B) Western blot analysis. Protein markers (lane 1); 20 μg of the BSA conjugate peptide (lane 2); 20 μg of human tropoelastin containing the exon 26A (lane 3); 20 μg of carbonic anhydrase (lane 4).

molecules but as an average result between folded and unfolded regions within the same peptide.

Quite interestingly, a recombinant human tropoelastin variant, lacking the hydrophilic sequence coded by exon 26A, has been reported to exhibit a marked increase of the Michaelis constant, when tested as a substrate for lysyl oxidase, relative to the isoform containing the complete sequence. It is suggested that the decrease in the apparent affinity for lysyl oxidase caused by the deletion "reflects ... specific changes in secondary or higher ordered degrees of structure of the tropoelastin isoforms" (*16*). In this context, it is tempting to suggest that the stable type II β-turn, spanning the sequence REGD, is indeed responsible for the increased binding to lysyl oxidase.

The cross-reactivity of the anti-CREGDPSSSQHLPSTPSSPRV antibodies with recombinant tropoelastin containing the sequence coded by exon 26A (Figure 6) confirms the presence of an epitope in this region and indicates that

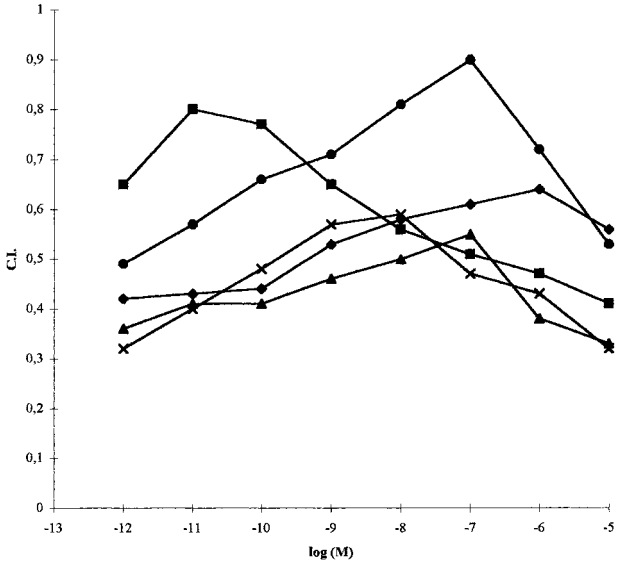

FIGURE 7: Chemotactic activity of human monocytes toward REGD (●); LREGDPSS (■); LPSTPSSP (▲); SSSQHLPS (×); and REGDPSSSQHLPSTPSSPRV (◆). The points are means of four to six separate experiments. SE are within 10% of the mean value. A chemotactic index of 0.92 ± 0.03 SE was observed for peak response migration of fMPL at 10^{-8} M.

Table 2: Monocyte Migration as Chemokinetic Activity (in the absence of a concentration gradient of peptides)[a]

log [M]	pep20	pep8a	pep8b	pep8c	REGD
−12	0.42	0.65	0.36	0.32	0.49
−11	0.43	0.80	0.41	0.40	0.57
−10	0.44	0.77	0.43	0.48	0.66
−9	0.53	0.65	0.46	0.57	0.71
−8	0.58	0.56	0.50	0.59	0.81
−7	0.61	0.51	0.55	0.47	0.90
−6	0.64	0.47	0.38	0.43	0.72
−5	0.56	0.41	0.33	0.32	0.53

[a] pep20, REGDPSSSQHLPSTPSSPRV; pep8a, LREGDPSS; pep8b, SSSQHLPS; pep8c, LPSTPSSP. The points are mean of 4−6 separate experiments. SE are within 10% of the mean value.

our polyclonal preparation is suitable for the identification of this sequence in different tissues by immuno-histochemical techniques.

It is known that several elastin peptides show chemotactic activity for fibroblasts, monocytes, and tumor cells and that this activity is mediated by the elastin laminin receptor that binds hydrophobic peptides, such as the hexapeptide VGVAPG and some other peptides studied by us (*5*, *7*, *49*). The chemotactic peptides REGD and LREGDPSS (Figure 7) are different from the peptides mentioned above, but present strong similarity, in terms both of primary and secondary structure, with the chemotactic RGD peptides that bind the integrin receptor; in fact, both RGD and REGD exhibit a type II β-turn (*48*). This structural and functional analogy with the integrin binding peptides suggests that exon 26A of human elastin may play a role in cellular adhesion. The definite biological significance of this exon will presumably be clarified when the tissues in which and the conditions, both physiological and pathological, under which the exon 26A is expressed will be known.

At present it has been reported that exon 26A is expressed in pulmonary hypertension (*18*), a pathological condition in which pulmonary arteries are affected by gross atherosclerotic

lesions and a marked thickening of the intima. In this tissue, the elastin isoform containing the exon 26A sequence is produced by the intimal cells and remains associated with the cell surface without being incorporated into the insoluble matrix. Furthermore, in the neointima of this pathological tissue there are macrophages which play an active role in the regulation of extracellular matrix gene expression (*50*). It is at present unknown how peripheral blood monocytes are recruited to the neointima. The chemotactic activity for monocytes exhibited by the peptides containing the sequence REGD reported in this paper is consistent with the hypothesis that exon 26A may play an active role in the migration of monocyte/macrophage cells to the neointima.

REFERENCES

1. Franzblau, C., Sinex, F. M., Faris, B., and Lanpidis, R. (1965) *Biochem. Biophys. Res. Commun. 21*, 525−531.
2. Partridge, S. M., Elsden, D. R., Thomas, J., Dorfman, A., Telser, A., and Ho, P. (1966) *Nature 20*, 399−400.
3. Hunninghake, G. W., Davidson, J. M., Rennard, S., Srapiel, S., Gradek, J. E., and Crystal, R. G. (1981) *Science 212*, 925−927.
4. Senior, R. M., Griffin, G. L., Mecham, R. P., Wrenn, D. S., Prasad, K. U., and Urry, D. W. (1984) *J. Cell. Biol. 99*, 870−874.
5. Mecham, R. P., Hinek, A., Entwistle, R., Wrenn, D. S., Griffin, G. L., and Senior R. M. (1989) *Biochemistry 28*, 3716−3722.
6. Bisaccia, F., Castiglione Morelli, M. A., De Biasi, M., Traniello, S., Spisani, S., and Tamburro, A. M. (1994) *Int. J. Pept. Protein Res. 35*, 81−88.
7. Blood, H. C., Sasse, J., Brodt, P., and Zetter, B. R. (1988) *J. Cell Biol. 107*, 1987−1994.
8. Indik, Z., Yeh, H., Ornstein-Goldstein, N., Sheppard, P., Anderson, N., Rosenbloom, J. C., Peltonen, L., and Rosenbloom J. (1987) *Proc. Natl. Acad. Sci. U.S.A. 84*, 5680−5684.
9. Raju, K., and Anwar, R. A. (1987) *J. Biol. Chem. 262*, 5755−5762.
10. Bressan, G. M., Argos, P., and Stanley, K. K. (1988) *Biochemistry 26*, 1497−1503.
11. Pierce, R. A., Deak, S. B., Stolle, C. A., and Boyd C. D. (1990) *Biochemistry 29*, 9677−9683.
12. Mauch, J. C., Sandberg, L. B., Ross, P. J., Jimenez, F., Christiano, A. M., Deak, S. B., and Boyd C. D. (1994) *Matrix Biol. 14*, 635−641.
13. Wydner, K. S., Sechler, J. L., Boyd, C. D.; Passmore, H. C. (1994) *Genomics 23*, 125−131.
14. Bashir, M. M., Indik, Z., Yeh, H., Ornstein-Goldstein, N., Rosenbloom, J. C., Abrams, W., Fazio, M., Uitto J., and Rosenbloom J. (1989) *J. Biol. Chem. 264*, 8887−8891.
15. Yeh, H., Ornstein-Goldstein, N., Indik, Z., Sheppard, P., Anderson, N., Rosenbloom, J. C., Cicilla, G., Yoon, K., and Rosenbloom, J. (1987) *Collagen Relat. Res. 7*, 235−247.
16. Bedell-Hogan, D., Trackman, P., Abrams, W., Rosenbloom, J., and Kagan, H. (1993) *J. Biol. Chem. 268*, 10345−10350.
17. Debelle, L., Wei, S. M., Jacob, M. P., Hornebeck, W., and Alix, A. J. P. (1992) *Eur. Biophys. J. 21*, 321−329.
18. Liptay, M. J., Botney, M. D., Mecham, R. P., Rosenbloom, J., Cooper, J. D., and Kaiser, L. R. (1991) *Surgical Forum*; Vol. XLII, pp 287−289, reprinted from American College of Surgeons.
19. Kadkhodaei, M., Hwang, T. L., Tang, J., and Shaka, A. J. (1993) *J. Magn. Reson. 105*, 104−107.
20. Macura, S., and Ernst, R. R. (1980) *Mol. Phys. 41*, 95−117.
21. Bothner-By, A. A., Stephens, R. L., Lee, J., Warren, C. D., and Jeanloz, R. W. (1984) *J. Am. Chem. Soc. 106*, 811−813.
22. Neidig, K. P., Geyer, M., Goerler, A., Antz, C., Saffrich, R., Beneicke, W., and Kalbitzer, H. R. (1985) *J. Biomol. NMR 6*, 255−270.
23. Macura, S., Farmer, B. T., and Brown, L. R. (1986) *J. Magn. Reson. 70*, 493−499.
24. Esposito, G., and Pastore, A. (1988) *J. Magn. Reson. 76*, 331−336.
25. Guentert, P., Braun, W., Billeter, M., and Wuethrich, K. (1989) *J. Am. Chem. Soc. 111*, 3997−4004.
26. Wuethrich, K., Billeter, M., and Braun, W. (1983) *J. Mol. Biol. 169*, 949−961.
27. Guentert, P., Braun, W., and Wuethrich, K. (1991) *J. Mol. Biol. 217*, 517−530.
28. Weiner, P. K., and Kollman, P. A. (1981) *J. Comput. Chem. 2*, 287−303.
29. Koradi, R., Billeter, M., and Wuethrich, K. (1996) *J. Mol. Graphics 14*, 51−55.
30. Scheidtmann K. H. (1989) In *Protein Structure, a Practical Approach*; Creighton T. E., Ed.; IRL Press: Oxford, U.K., pp 93−115.
31. Boulay, F., Lauquin, G. J. M., and Vignais, P. V. (1986) *Biochemistry 25*, 7567−7571.
32. Towbin, H., Staehelin, T., and Gordon, J. (1979) *Proc. Natl. Acad. Sci. U.S.A. 76*, 4350−4354.
33. Laemnly, U. K. (1979) *Nature 227*, 680−685.
34. Zigmond, S. H., and Hirsch, J. G. (1973) *J. Exp. Med. 137*, 387−391.
35. Spisani, S., Traniello, S., Giuliani, A. L., Torrini, I., Pagani Zecchini, G., Paglialunga Paradisi, M., Gavuzzo, E., Mazza, F., Pochetti, G., and Lucente, G. (1992) *Biochem. Int. 26*, 1125−1135.
36. Wuethrich, K. (1986) *NMR of Proteins and Nucleic Acids*; Wiley: New York.
37. Wishart, D. S., Sykes, B. D., and Richards, F. M. (1991) *J. Mol. Biol. 222*, 311−333.
38. Wishart, D. S., Sykes, B. D., and Richards, F. M. (1992) *Biochemistry 31*, 1647−1651.
39. Wilce, J. A., Zeng, W., Rose, K., and Craik, D. J. (1996) *Biomed. Pept. Proteins Nucleic Acids 2*, 51−58.
40. Dyson, H. J., Rance, M., Houghten, R. A., Wright, P. E., and Lerner, R. A. (1988) *J. Mol. Biol. 201*, 201−217.
41. Tamburro, A. M., Scatturin, A., Rocchi, R., Marchiori, F., Borin, G., and Scoffone, E. (1968) *FEBS Lett. 1*, 298−300.
42. Mammi, S., Mammi, N. J., and Peggion, E. (1988) *Biochemistry 27*, 1374−1379.
43. Nelson, J. W., and Kallenbach, N. R. (1989) *Biochemistry 28*, 5256−5261.
44. Soennichsen, F. D., Van Eyk, J. E., Hodges, R. S., and Sykes, B. D. (1992) *Biochemistry 31*, 8790−8797.
45. Dyson, H. J., and Wright, P. E. (1991) *Annu. Rev. Biophys. Chem. 20*, 519−538.
46. Perczel, A., Hollosi, M., Sandor, P., and Fasman G. D. (1993) *Int. J. Pept. Protein Res. 41*, 223−236.
47. Marastoni, M., Salvadori, S., Balboni, G., Spisani, S., Gavioli, R., Traniello, S., and Tomatis, R. (1990) *Int. J. Pept. Protein Res. 35*, 81−88.
48. Curtis, J. W., Jr., Pagano, T. G., Basson, C. T., Madri, J. A., Gooley, P., and Armitage, I. M. (1993) *Biochemistry 32*, 268−273.
49. Castiglione Morelli, M. A, Bisaccia, F., Spisani, S., De Biasi, M., Traniello, S., and Tamburro, A. M. (1997) *J. Peptide Res. 49*, 492−499.
50. Liptay, M. J., Parks, W. C., Mecham, R. P., Roby, J., Kaiser, L. R., Cooper, J. D., and Botney, M. D. (1993) *J. Clin. Invest. 91*, 588−594.

BI9802566